Int. J. Electrochem. Sci., 12 **(2017)** 8188 – 8197, doi: 10.20964/2017.09.62

International Journal of
ELECTROCHEMICAL
SCIENCE
www.electrochemsci.org

Ultrasensitive Electrochemical Detection of Prostate-Specific Antigen (PSA) Based on Graphene-Silver Nanocomposite

Lei Yu[1], *Zhen Fan*[2], *Wenxian Li*[3], *Shenqian Li*[1], *Peitao Wang*[1] *and Hongqiang Wang*[1,*]

[1] Department of Andrology, The Affiliated Hospital of Qingdao University, No.16 Jiangsu Road, Shinan District, Qingdao City, Shandong Province, 266000, P.R. China
[2] Department of Ophthalmology, Qingdao Haici Medical Group, Qingdao City, Shandong Province, 266000, P.R. China
[3] Department of Urology, The Affiliated Hospital Of Qingdao University, No.16 Jiangsu Road, Shinan District, Qingdao City, Shandong Province, 266000, P.R. China
[*]E-mail: hongqiangwangsally@qq.com

Received: 5 June 2017 / *Accepted:* 27 July 2017 / *Published:* 13 August 2017

In this work, the electrostatic layer-by-layer (LbL) assembly of bovine serum albumin (BSA) functionalized graphene nanosheets and silver nanoparticle (AgNP), along with the thermal annealing at 340 °C in air were performed to prepare a thin and uniform film of AgNP–embedded porous graphene (AgEPG). To determine prostate specific antigen (PSA) in human serum, we proposed a new electrochemical immunosensor based on a protein tracer, namely the functionalized AgEPG. Our proposed immunosensor was feasible to detect PSA (1–35 ng/mL) under optimal electrochemical and immunoreactions determination conditions, and the limit of detection (LOD) was calculated as 0.44 ng/mL.

Keywords: Prostate-specific antigen; Electrochemical sensor; Graphene; Silver; Children asthmatic Layer-by-layer

1. INTRODUCTION

As a 32–33-kDa single-chain glycoprotein, prostate specific antigen (PSA) has obtained substantial attention in the last few years, and proved to be excellent as a tumor marker used for the early-stage prostate cancer determination at organ-confined stage, and for the monitoring of disease recurrence after treatment [1-3]. Normally PSA could be detected in serum at trace level. However, the growth of prostate cancer tumor often leads the PSA at high concentrations to release to the circulation system. A PSA test beyond the critical value (4 ng/mL) was initially considered positive, possibly suggesting the necessity of a biopsy [4]. Thus is of great clinical importance to propose fast, sensitive

and facile immunoassay techniques to detect the concentration of PSA in serum in prostate cancer diagnostics.

Despite nucleic acids involved in several techniques for the determination of PSA [5], a majority of techniques for PSA determination are based on varying determination protocols. Sandwich-type enzyme-linked immunosorbent assay (ELISA), the initial immunoassay for PSA, was proposed by Kuriyama and co-workers [6]. Afterwards, other ELISA immunoassays for PSA were developed. Then other detection methods using surface enhanced Raman scattering (SERS), immunochromatography, surface plasmon resonance (SPR) and fluorescence microscopy were proposed [7-10]. Besides, some commercial immunoassays have been reported for the total PSA detection clinically, using large automatic high-throughput systems for centralized laboratory experiment including Diagnostic Products Corporation's Immulite assay, Abbott's IMx assay and Roche's Elecsys assay [4]. Nevertheless, new biosensor determination techniques for miniaturized PSA detection have been proposed due to the focus on the demand for point-of-care (POC) patient management. The immunosensor format, where PSA binding was achieved using high-affinity antibodies to yield the recognition element of the apparatus, was widely employed to prepare the biosensors for PSA detection.

The self-contained apparatus containing a physicochemical transducer was prepared using molecular recognition elements (immunochemicals) in immunosensor technology. Due to the high affinity constants of the antigen–antibody interactions, most of them are single-use systems. Although ordinarily immunosensors are highly sensitive and selective, their applications have not been considered successful, since they are unstable, not much reproducible, and require to be added with external reagents. Based on previous literatures, optical (fluorescence, laser-based) [11], electrochemical [12-15] and piezoelectric [16-18] transduction modes have been proposed to be involved in many immunosensor fabrications for PSA determination.

Since graphene–metal nanoparticle has great potential to be used in sensors [19-27], fuel cells [28, 29] and energy conversion [29], they have been extensively studied recently. Graphene has been accepted as a remarkable substrate for metal nanoparticle immobilization, due to its distinct features of its two-dimensional (2D) exfoliated graphene sheets, including low construction cost, high mechanical strength, desirable charge mobility, large surface area, etc. There have been substantial improvements in the preparation of the 2D graphene–metal nanoparticle hybrids [30, 31]. Nevertheless, there are still many tough issues to deal with. For instance, in order for the molecular-scale and macroscopic-scale assembly of the above nanohybrids to be integrated to apparatus structures, they have to be adjusted. With respect to large numbers of utilities, the spatial distribution as well as the orientation of graphene–metal nanoparticle hybrids required to be controlled [32, 33]. A couple of techniques have been employed for the preparation of large-scale assembled graphene hybrid films to deal with the above issue [34]. The LbL assembly is more efficient and facile than its counterparts, since it could precisely control the thickness and structure of the films either on the nanoscales and microscales [29]. In recent years, the LbL assembly strategy was used for the preparation of three-dimensional (3D) hybrid films based on the combination of metal nanoparticles and a building block (graphene nanosheet) [33].

In this study, electrostatic LbL assembly of BSA - functionalized graphene nanosheets and AuNPs, along with following thermal annealing at 340 °C in air were performed for the preparation of a new and thin AgNP–embedded porous graphene (AgEPG) film using a simple and novel technique. The 1-ethyl-3-(dimethylaminopropyl) carbodiimide hydrochloride (EDC)/*N*-hydroxysuccinimide (NHS) crosslink was employed for the synthesis of the functionalized AgEPG and detection antibody. After sandwich type immunocomplex consisting of capture antibody, antigen and functionlized AuEPG was formed on the surface of the electrode, the ascorbic acid was converted from the ascorbic acid 2-phosphate (AA-P) by the ALP present on the AgEPG. Afterwards the silver was deposited on the surface of the electrode through the reduction of Ag(I) ions in the solution. Afterwards, linear sweep voltammetry (LSV) was performed to obtain the amount of deposited silver.

2. EXPERIMENTS

2.1. Chemicals

A pair of mouse monoclonal antibodies was purchased from T.J. Biotechnologies (Tianjin), Ltd. (China), and employed in the sandwich immunoassay. The detection antibody and the capture antibody were the mouse anti-human total PSA clone PSA103, and mouse anti-human total PSA clone PSA140, respectively. Total PSA was commercially available in Beijing Institute of Materia Medica and Biological Products (Beijing, China). BSA was commercially available in Beijing Dingguo Biotechnology Development Center (China). Alkaline phosphatase (calf intestinal) was commercially available in Promega Corporation (USA). Poly(ethylenimine) (PEI, 50% in water, M_w = 750 000 by LS) was commercially available in from Sigma–Aldrich. Graphite powder (99.9%, 325 mesh) and $AgNO_3$ were commercially available in Alfa Aesar.

2.2. Apparatus

A model CHI660C electrochemical workstation (Shanghai Chenhua Instruments, Shanghai, China) linked to a personal computer was used for all electrochemical tests. The traditional triple-electrode electrochemical configuration was employed, where the working electrode was a 99.99% gold material (diameter: 4 mm), the reference electrode was a KCl saturated calomel (SCE), and the counter electrode was a platinum wire. All potentials were referenced to the reference electrode. The three electrodes were all available in Shanghai Chenhua Equipments. The maternal serum PSA was measured either by chemiluminescent microparticle immunoassay (CMIA) (Architect i2000 analyzer; Abbott Diagnostics, Abbott Park, IL, USA). With respect to the linear sweep voltammetric tests, the scanning rate was 100 mV/s, and the potential ranged from 0 to 0.8 V (vs. SCE). The supporting electrolyte for the electrochemical tests was a 0.6 M KNO_3 solution + 0.1 M HNO_3. The test was performed at ambient temperature.

2.3. Preparation of PEI/BSA-G/(BSA-G$^+$/AuNPs)$_n$ Multilayer Films

The multilayer film was prepared on the substrates, namely the FTO electrodes or quartz slides. The quartz slide was pre-treated in hot piranha solution (7:3 v/v) composed of H_2O_2 (30%) and H_2SO_4 (98%) for ca. 0.5 h, followed by water washing. FTO was sonicated sequentially using acetone, KOH (10%) in ethanol, and H_2O, for 20 min, respectively, for cleaning. After immersing the freshly cleaned FTO electrode or quartz slide with 2.5 mg/mL PEI solution for 20 min, they were rinsed using water and dried under N_2. Afterwards, the surface was negatively charged after immersing the PEI-decorated electrode into the BSA-G suspension for 20 min. The as-prepared substrate was washed and dried under N_2 (denoted as PEI/BAS-G), alternately immersed in AgNPs and BSA-G$^+$ suspensions each for 20 min, and then washed and dried using the same process (denoted as PEI/BSA-G/(BSA-G$^+$/AgNPs). The PEI/BSA-G/(BSA-G$^+$/AgNPs)$_n$ film was finally obtained after the depositions between AuNPs and BSA-G$^+$ repeated, and then introduced into a furnace, followed by annealing in air at varying temperatures in air for 120 min. The AgEPG film was finally produced after annealing for 120 min at 340 °C.

2.4. Preparation of antibody-modified gold electrode

The self-assembled monolayer (SAM) was prepared by immersing the AgEPG into 10 mM cysteamine aqueous solution for ca. 12 h. The adsorbed cysteamine was removed after completely rinsing the electrode into water. Then the as-prepared electrode was soaked into a 2.5% (w/w)glutaraldehyde aqueous solution at 37 °C for 60 min, followed by further washing using water. Afterwards, an aliquot (10-μL) of capture antibody (100 μg/mL) was dropped onto the as-prepared electrode, followed by incubation at 37 °C for 60 min, and intensive washing using PB buffer and water. To obstruct the unreacted aldehyde, the as-prepared electrode was incubated with BSA (0.3%) in PB buffer (0.03 mM) for 60 min. A range of specimens (10 μL) that contained varying concentrations of purified PSA antigen or serum were used for the incubation (37 °C; 60 min)of the electrodes modified by the capture antibody. This was followed by incubating the as-prepared electrodes in the freshly synthesized glycine buffer solution (50 mM; pH 9.08) that contained AA-P (1 mM) and $AgNO_3$ (1 mM) for 35 min at 37 °C. Finally the as-incubated electrode was rinsed using ultrapure water.

3. RESULTS AND DISCUSSION

The building block was citrate-stabilized AuNPs. The electrostatic interactions – based LbL assembly entailed positively charged graphene nanosheets, considering the negatively charged citrate-stabilized AuNPs. The highly dispersed functionalized reduced GO solutions were synthesized using a reduction and decoration agent - BSA. BSA has previously been shown to be an effective reagent for the reduction of graphene oxide since the phenolic groups in its tyrosine (Tyr) residues can be readily oxidized to quinone groups [35]. As shown in Fig. 1, the PEI/BSA-G/(BSA-G+/AgNPs)$_5$ film was

characterized cia the XRD profile, confirming that graphene and AgNPs were present in the assembled film. The above results suggested the successful synthesis of a uniform multilayer film on the graphene/AgNP composite.

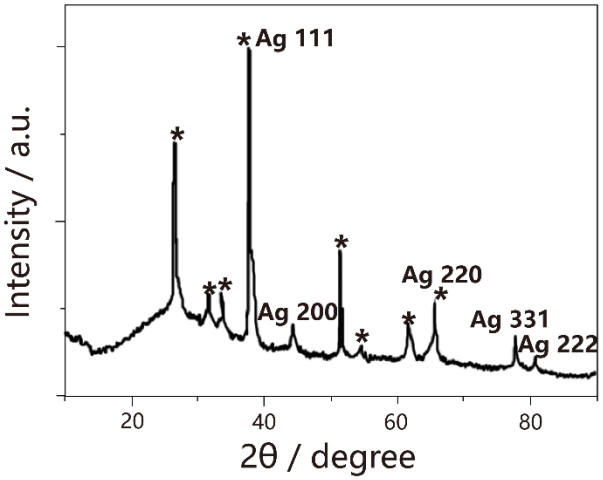

Figure 1. XRD profile of PEI/BSA-G/(BSA-G+ /AgNPs)$_5$ film on a FTO slide.

BSA on the graphene nanosheets surface was decomposed after introducing the thermal annealing treatment, thus improving the conductivity of the PEI/BSA-G/(BSA-G$^+$/AgNP)$_5$ film in electrochemical utilities. Firstly, the multilayer film was thermally annealed under N_2 at 400 °C. However, compared with the electrode modified by nonannealed film, the FTO electrode modified by PEI/BSA-G/(BSA-G$^+$/AgNP)$_5$ showed no obvious enhancement in its electrochemical features. Afterwards, we performed the thermal annealing procedure. Fig. 2 showed the TGA of BSA, BSA-G, and BSA-G/AgNP hybrids in air. When the temperature exceeded 250 °C, BSA in the BSA-G/AgNP hybrids was observed to be decomposed. The apparent decomposition of the graphene occurred at the temperature > 450 °C. Hence we set 300 - 450 °C as the temperature range for thermal annealing.

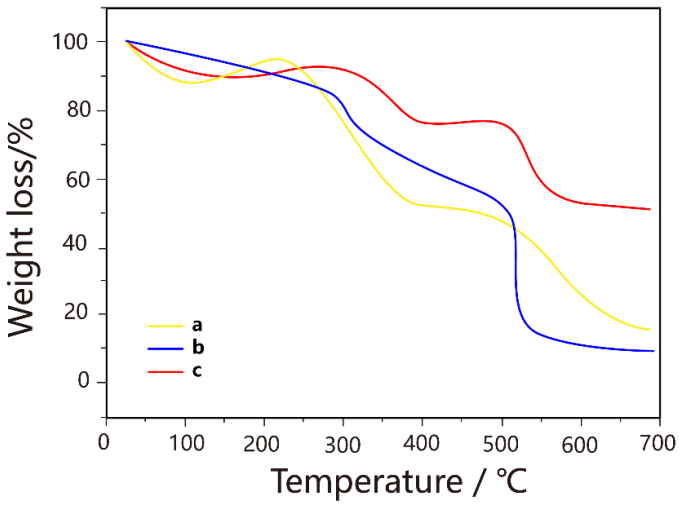

Figure 2. TGA profiles of (a) BSA, (b) BSA-G and (c) BSA-G/AgNP hybrids in air.

In order to confirm the successful modification of the AgEPG by the ALP and the detection antibody, we further carried out the electrochemical immunoassay. PSA (35 ng/mL) was determined using the unmodified AgEPG, as well as the ALP and detection antibody labeled AgEPG, respectively. As displayed in Fig. 3, the unmodified AgEPG exhibited no obvious LSV readout, whereas the ALP and detection antibody labeled AgEPG showed a stripping peak current (ca. 160 μA). On the other hand, phosphate buffer rather than the target protein was determined using the modified AgEPG, with insignificant peak current observed in the LSV assay. The above results verified the successful modification of the AgEPG by the ALP and the detection antibody.

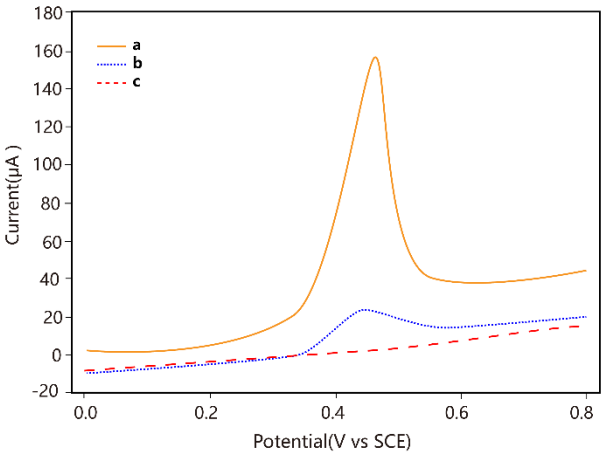

Figure 3. LSV readouts of enzymatically deposited electrodes in KNO_3 (0.6 M)/HNO_3 (0.1 M) solutions. The results of the detection antibody and ALP labelled AgEPG were shown in Profiles (a) and (b) for the determination of target protein PSA and phosphate buffer, respectively. The results of the unmodified AgEPG were shown in Curve (c) for the determination of target protein PSA.

The amount of ALP attached on the surface of the electrode was found to determine the amount of biocatalytically deposited metal silver. The surface modification was carried out at the ALP concentration of 100 - 600 U/mL, and the PSA detection antibody concentration of 100 μg/mL. Apparently, the more the amount of ALP carried on per nanocomposite, the higher is the sensitivity of the electrochemical immunosensor. The detection antibody competed with the ALP to react with the fixed and limited number of carboxyl on the surface of the AgEPG. As indicated in Fig. 4, the effect of the concentration of ALP for the functionalization of AgEPG present on the anodic stripping peak current (ASPC) was studied. With the range of the ALP of 100 - 400 U/mL, an obvious increase in ASPC was observed, which subsequently decreased when the ALP concentration further increase to 600 U/mL. With the increase in the ALP concentrations in solution (100 - 400 U/mL), an increase in the amount of ALP modified on the AgEPG surface was observed, then the stripping peak current (SPC) of our proposed immunosensor ascended. On the contrary, when the amount of ALP in modified solution is much larger than the amount of the detection antibody, the competition of the detection antibody and ALP induces that the amount of antibody attached on the surface of nanocomposite is relatively small, which results in the decrease in the stripping peak currents because the sandwich immunocomplex could not be formed well on the electrode surface [36]. Therefore, we set 400 U/mL

as the optimum ALP concentration for functionalization in following tests. As shown in Fig. 4B, the effect of deposition time of biocatalytic silver on the SPC was studied. Within the initial 35 min of deposition, the rapid increase in the peak current was observed. Then the current showed a slow increase tendency. This phenomenon may be associated with the loss of the enzyme activity with the increase in the deposition time [35]. Hence 35 min was selected as the optimum deposition time for the biocatalytic reaction.

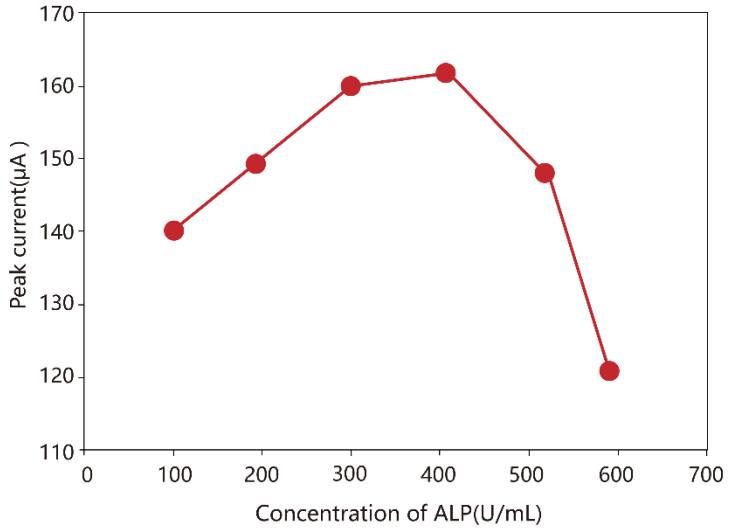

Figure 4. (A) Effect of the concentration of ALP for the AgEPG functionalization on the ASPC. (B) Effect of the biocatalytic silver deposition time on the ASPC.

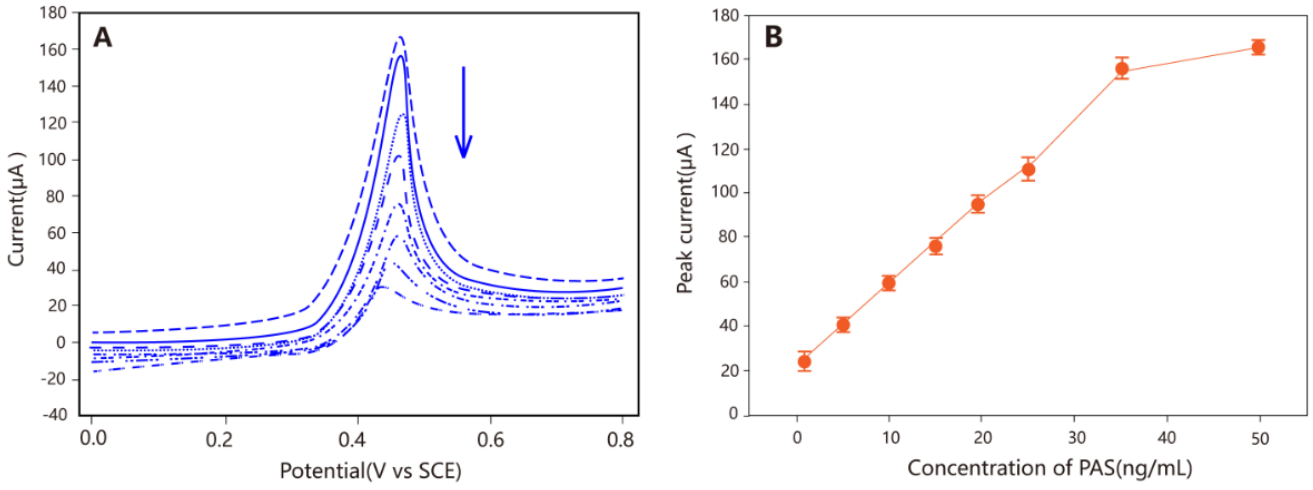

Figure 5. (A) LSVs of the electrochemical immunosensors in KNO_3 (0.6 M)/HNO_3(0.1 M) solution at a target protein concentrations of 35, 25, 20, 15, 5, 1 and 0.5 ng/mL. (B) Calibration profile of peak current as a function of target protein concentration with the electrochemical immunosensor.

Table 2. PSA determination performance comparison between PEI/BSA-G/(BSA-G^+/AgNP)$_5$ and other reports.

Detection method	LR (ng/mL)	DL (ng/mL)	Reference
Screen-printed electrode	0.01-1	0.002	[37]
Organic electrochemical transistor based immunosensor	—	0.004	[38]
Ferrocene-functionalized peptide probes	0.5-40	0.2	[39]
PEI/BSA-G/(BSA-G^+/AgNP)$_5$	0.5-35	0.44	This work

In this work, we studied a range of target analyte with varying concentrations for the calibration profile. The LSV responses of our proposed immunosensor toward a range of concentrations of target analyte were characterized in Fig. 5A. It can be seen that the SPC of our proposed immunosensor increased with the increasing target analyte concentration. Our proposed immunosensor was also characterized via calibration profile, as shown in Fig. 5B. It can be seen that the target analyte concentration (1-35 ng/mL) was linearly related with the SPC of our proposed immunosensor. And LOD was calculated as 0.44 ng/mL (S/N=3). And saturation occurred at the target analyte concentration of over 35 ng/mL, probably since the antibodies immobilized on the surface of the electrode was completely bound. The results of PSA content determination in these serum samples were showed in Table 1. As shown, the PEI/BSA-G/(BSA-G^+/AgNP)$_5$ has an excellent performance of CK detection for real samples. Additionally, we have compared this electrode with some other modified electrodes for the determination of CK, as summarized in Table 1.

Table 2. The comparisons of the proposed electrochemical immunosensora (EI) using the chemiluminescent microparticle immunoassay (CMIA) strategy for the determination of PSA in human serum

Serum sample	EI (ng/mL)	CMIA (ng/mL)	Relative deviation (%)
1	2.75	2.69	2.45
2	6.03	6.01	3.62
3	6.65	6.78	1.05
4	6.55	6.49	0.78
5	10.22	10.18	2.51

Five measurements were carried out with the same procedures for the assessment of the reproducibility of the electrochemical immunosensor, with a relative standard deviation (RSD) of 2.8%, suggesting the remarkable reproducibility of our developed immunosensor in preparation and measurement.

The proposed immunosensor was used to investigate five human serum samples so as to study the applicability of it to clinical detection. Meanwhile, the chemiluminescent microparticle immunoassay (CMIA) was also used herein as a reference strategy. Based on the results in Table 2, the concentrations of the target analyte recorded using our proposed technique were consistent with those of the CMIA strategy (relative deviations < 3.62%), suggesting the feasibility of our proposed immunosensor to be used for the detection of PSA in human serum specimens.

4. CONCLUSIONS

In this work, LbL assembly, together with thermal annealing in air, were used to prepare a uniform and new AgEPG film. And AgEPG was used to fabricate the ultrasensitive electrochemical immunosensor to detect human PSA. Due to biocatalytic deposition of metal silver and the ALP-functionalized AgEPG, the dual-signal amplification was achieved. And the low LOD was obtained as 0.44 ng/mL. Ascribed to the desirably developed AgEPG immobilization chemistry, the cofunctionalization technique could also be employed for varying biomolecules. In addition, other proteins could be determined using corresponding electrochemical immunosensors.

References

1. J. Walboomers, M. Jacobs, M. Manos, F. Bosch, J. Kummer, K. Shah, P. Snijders, J. Peto, C. Meijer and N. Munoz, *The Journal of Pathology*, 189 (1999) 12.
2. C. Fernández-Sánchez, C. McNeil, K. Rawson and O. Nilsson, *Anal. Chem.*, 76 (2004) 5649.
3. C. Fernández-Sánchez, A. Gallardo-Soto, K. Rawson, O. Nilsson and C. McNeil, *Electrochemistry Communications*, 6 (2004) 138.
4. D. Healy, C. Hayes, P. Leonard, L. McKenna and R. O'Kennedy, *TRENDS in Biotechnology*, 25 (2007) 125.
5. S. Hoshi, S. Kobayashi, T. Takahashi, K. Suzuki, S. Kawamura, M. Satoh, Y. Chiba and S. Orikasa, *Urology*, 53 (1999) 228.
6. M. Kuriyama, M. Wang, L. Papsidero, C. Killian, T. Shimano, L. Valenzuela, T. Nishiura, G. Murphy and T. Chu, *Cancer Research*, 40 (1980) 4658.
7. K. Kerman, T. Endo, M. Tsukamoto, M. Chikae, Y. Takamura and E. Tamiya, *Talanta*, 71 (2007) 1494.
8. C. Cao, J. Kim, B. Kim, H. Chae, H. Yoon, S. Yang and S. Sim, *Biosensors and Bioelectronics*, 21 (2006) 2106.
9. T. Yuhi, N. Nagatani, T. Endo, K. Kerman, M. Takata, H. Konaka, M. Namiki, Y. Takamura and E. Tamiya, *Science and Technology of Advanced Materials*, 7 (2006) 276.
10. D. Grubisha, R. Lipert, H. Park, J. Driskell and M. Porter, *Anal. Chem.*, 75 (2003) 5936.
11. P. O'Neill, J. Fletcher, C.G. Stafford, P.B. Daniels and T. Bacarese-Hamilton, *Sensors and Actuators B: Chemical*, 29 (1995) 79.
12. P. Sarkar, P. Pal, D. Ghosh, S. Setford and I. Tothill, *International Journal of Pharmaceutics*, 238 (2002) 1.
13. P. Sarkar, D. Ghosh, D. Bhattacharyay, S. Setford and A. Turner, *Electroanalysis*, 20 (2008) 1414.
14. N. Panini, G. Messina, E. Salinas, H. Fernández and J. Raba, *Biosensors and Bioelectronics*, 23 (2008) 1145.
15. Y. Liu, *Thin Solid Films*, 516 (2008) 1803.

16. J. Lee, K. Hwang, J. Park, K. Yoon, D. Yoon and T. Kim, *Biosensors and Bioelectronics*, 20 (2005) 2157.
17. B. Zhang, X. Zhang, H.-h. Yan, S. Xu, D. Tang and W. Fu, *Biosensors and Bioelectronics*, 23 (2007) 19.
18. Y. Ding, H. Lu, G. Shi, J. Liu, G. Shen and R. Yu, *Biosensors and Bioelectronics*, 24 (2008) 228.
19. S. Guo, D. Wen, Y. Zhai, S. Dong and E. Wang, *ACS Nano*, 4 (2010) 3959.
20. S. Myung, A. Solanki, C. Kim, J. Park, K.S. Kim and K.B. Lee, *Adv. Mater.*, 23 (2011) 2221.
21. M. Yola, T. Eren and N. Atar, *Sensors and Actuators B: Chemical*, 210 (2015) 149.
22. Y. Zhang, G.M. Zeng, L. Tang, J. Chen, Y. Zhu, X. He and Y. He, *Anal. Chem.*, 87 (2015) 989.
23. X. Feng, Y. Zhang, J. Zhou, Y. Li, S. Chen, L. Zhang, Y. Ma, L. Wang and X. Yan, *Nanoscale*, 7 (2015) 2427.
24. A. Lawal, *Talanta*, 131 (2015) 424.
25. X. Luo, J. Pan, K. Pan, Y. Yu, A. Zhong, S. Wei, J. Li, J. Shi and X. Li, *Journal of Electroanalytical Chemistry*, 745 (2015) 80.
26. X. Zhang, L. Wu, J. Zhou, X. Zhang and J. Chen, *Journal of Electroanalytical Chemistry*, 742 (2015) 97.
27. S. Dong, J. Xi, Y. Wu, H. Liu, C. Fu, H. Liu and F. Xiao, *Anal. Chim. Acta.*, 853 (2015) 200.
28. E. Yoo, T. Okata, T. Akita, M. Kohyama, J. Nakamura and I. Honma, *Nano Letters*, 9 (2009) 2255.
29. Q. Xi, X. Chen, D. Evans and W. Yang, *Langmuir*, 28 (2012) 9885.
30. W. Zhang and H. Choi, *Chemical Communications*, 47 (2011) 12286.
31. X. Chen, G. Wu, J. Chen, X. Chen, Z. Xie and X. Wang, *Journal of the American Chemical Society*, 133 (2011) 3693.
32. H. Bai, C. Li and G. Shi, *Adv. Mater.*, 23 (2011) 1089.
33. C. Zhu, S. Guo, Y. Zhai and S. Dong, *Langmuir*, 26 (2010) 7614.
34. Q. Ji, I. Honma, S.M. Paek, M. Akada, J.P. Hill, A. Vinu and K. Ariga, *Angewandte Chemie*, 122 (2010) 9931.
35. H. Jang, S. Kim, H. Chang and J. Choi, *Biosensors and Bioelectronics*, 63 (2015) 546.
36. Z. Yang, B. Kasprzyk-Hordern, S. Goggins, C. Frost and P. Estrela, *The Analyst*, 140 (2015) 2628.
37. M. Yan, D. Zang, S. Ge, L. Ge and J. Yu, *Biosensors and Bioelectronics*, 38 (2012) 355.
38. D. Kim, N. Lee, J. Park, I. Park, J. Kim and H. Cho, *Biosensors and Bioelectronics*, 25 (2010) 2477.
39. N. Zhao, Y. He, X. Mao, Y. Sun, X. Zhang, C. Li, Y. Lin and G. Liu, *Electrochemistry Communications*, 12 (2010) 471.